BioMetals (2006) 19:245–251
DOI 10.1007/s10534-005-6666-2

Age-associated iron accumulation in bone: Implications for postmenopausal osteoporosis and a new target for prevention and treatment by chelation

Gang Liu*, Ping Men, Gerry H. Kenner & Scott C. Miller
*Radiobiology Division, Department of Radiology, School of Medicine, University of Utah, 729 Arapeen Dr. Suite 2334, Salt Lake City, UT, 84108, USA; *Author for correspondence (E-mail: gang.liu@m.cc.utah.edu)*

Received 13 January 2005; accepted 29 April 2005

Key words: aging, disease, chelator, metal, oxidative damage

Abstract

Iron accumulation in tissues is believed to be a characteristic of aged humans and a risk factor for some chronic diseases. However, it is not known whether age-associated iron accumulation is part of the pathogenesis of postmenopausal osteoporosis that affects approximately one out three women worldwide. Here, we confirmed that this accumulation of iron was associated with osteopenia in ovariectomized (OVX) rats (a model of peri- and postmenopausal osteoporosis due to estrogen deficiency). To further investigate whether the increased iron level plays a causal role in the onset of bone loss, we treated OVX rats with an orally active and bone targeted chelator that prevented iron accumulation in their skeletal tissues. The results showed that this treatment mitigated the loss of bone mass and the deterioration of bone microarchitecture. We also found that one possible mechanism of the protective action of iron chelation was to significantly reduce bone resorption. Thus, these findings provide a novel target and a potentially useful therapeutic strategy for the prevention and treatment of postmenopausal osteoporosis and perhaps other age-related diseases.

Introduction

Postmenopausal osteoporosis is a more dangerous disease than previously thought. The lifetime risk of dying from osteoporotic hip fractures alone (about 20% of all osteoporotic fractures) is the same as that of dying from breast cancer (Seidman *et al*. 1985; Cummings *et al*. 1989). The disease has a subtle progression and the etiology may be multifactorial and include genetic, endocrine, exercise, life-style and aging components (Raisz & Rodan 2003; Klein *et al*. 2004). Nutrition also plays an important role in the development of this disease (Department of Health 1998; Muhlbauer & Li 1999).

Iron is an essential nutrient for virtually all mammalian cells, but it is a double-edged sword. Excess iron is toxic, causing cellular dysfunction mainly due to being a powerful catalyst for the generation of highly toxic free radicals that can damage all molecular classes found *in vivo* (Halliwell & Gutteridge 1999). In aging, iron accumulates in tissues due to the lack of a major mechanism of iron excretion in the human body (McCance & Widdowson 1938). Stored body iron estimated by serum ferritin (SF) concentrations increases rapidly after menopause in women and adolescence in men (Howes *et al*. 2000). The increase continues with age and the iron stores appear to plateau about the sixth decade of life (Howes *et al*. 2000). In postmenopausal women, the average level of stored iron as reflected by SF concentrations, is about 106 ng/mL, more than twice that in pre-menopausal women at about 43 ng/mL (Kato *et al*. 2000). In adult men, the average concentration of SF is about 121 ng/mL while for males of 5 to 19 years of age it is about 20 to 30 ng/mL (The British Nutrition Foundation

1995). These age-associated increases in stored iron are considered to be moderate, compared to the pathological forms of primary and secondary iron overload (The British Nutrition Foundation 1995; Kato *et al.* 2000). However, these elevations are still, albeit controversial (Danesh & Appleby 1999), suggested to be risk factors for several chronic diseases such as atherosclerosis (Sullivan 1981), cancer (Stevens *et al.* 1988), diabetes (Woo *et al.* 1989) and metabolic disorders associated with the insulin resistance syndrome (Moirand et al. 1997).

While osteoporosis is common in postmenopausal women and tissue levels of iron are elevated in this population, the possible relationship between iron accumulation and osteoporosis has not been explored in this population. It was the purpose of this study to determine, in an animal model of estrogen-deficiency bone loss, the possible role of skeletal iron accumulation in the development of osteopenia. The results from this study indicate that iron may have a role in the pathogenesis of osteopenia with estrogen deficiency and as such a new pathway for the progression and possible treatment of this disease is identified.

Materials and methods

Animal and treatment

Three-month-old female Sprague-Dawley rats (Charles River Laboratory) were obtained and housed with 12 h light-dark cycles at constant room temperature (24°C) and humidity. The rats were fed standard rat chow (#8640 Harland Teklad) and water *ad libitum*. At six months of age, the rats were divided into four groups. One group was sacrificed as baseline controls at the beginning of the experiment. The remaining groups were sham operated (one group) or bilaterally ovariectomized (OVX) (two groups) via a dorsal approach. Chelation treatments started from the second day after surgery and were given three times a week for 9 weeks. The chelator (1-N-docosyl-triethylenetetraminepentaacetic acid) was dissolved in saline (pH 7.5) and was administered through oral gavage (100 μmol/kg). The control groups including the sham and OVX-operated were only given the vehicle solution in the same manner.

The fluorochrome bone markers calcein (fluorescein-methylene-iminodiacetic acid, 10 mg/kg body weight) and tetracycline-HCl (25 mg/kg body weight) from Sigma Chemical Co., were given by intraperitoneal injections on 10 and 3 days, respectively, prior to necropsy for later evaluation of bone dynamics by histomorphometry. The rats were anesthesized and sacrificed by cardiac puncture. The humerii and lumbar vertebrae were collected. The experiment was approved by the Institutional Animal Care and Use Committee.

Tissue preparation and analyses

Humeral bone samples were fixed in 70% ethanol for measurement of tissue iron by electron paramagnetic resonance (EPR). Lumbar vertebrae were first fixed in 10% phosphate buffered formalin for 24 h, then dehydrated in ascending concentrations of ethanol and embedded in methyl methacrylate. The blocks were trimmed for peripheral computed tomography (pQCT), micro-computed tomography (Micro-CT) and later prepared for histomorphometric studies.

pQCT densitometry

The third vertebral bodies were examined by pQCT densitometry (Norland Stratec XCT 960A) to determine bone mineral density (BMD) for the part from the middle point to caudal end excluding the primary spongiosa. A scout scan of the vertebra was performed. On the scout view, a reference line was set such that the cross-sectional slices passed through at a distance of 1, 2, 3 and 4 mm from the caudal end of the vertebra body. The voxel size was 196 mm. The contour-mode 2, peel-mode 20, cortical-mode 2 and threshold 570 for cortical bone were chosen for the analysis. The mean BMD for all of the measured slices was then calculated.

Micro-CT measurement

Lumbar vertebrae were scanned using a desktop Micro-CT (μCT-40, Scanco Medical) with a resolution of 10 μm in all three spatial dimensions. The complete third vertebral bodies were scanned with 600 slices, each slice containing 2048×2048 pixels. The trabecular and the cortical part of the bodies were separated with semi-automatically drawn contours. The resulting gray-scale images were segmented using a low-pass filter to remove

noise and a fixed threshold to extract the mineralized bone phase. From the binary images, structural indices were assessed with three-dimensional techniques without model-assumptions of the appearance of trabecular bone and were calculated by measuring three-dimensional distances directly in the trabecular network and taking the mean over all voxels. The region of interest was trabecular bone in the lumbar vertebral body excluding the primary spongiosa area, 0.5 mm from the growth plate (Laib *et al.* 2001).

Histomorphometric measurement

The third vertebral bodies were cut with a precision bone saw (Isomet, Buehler), the sections mounted on plastic slides and ground to about 30 μm in thickness. The sections were left unstained for viewing of the fluorochrome markers. The cancellous bone in one lumbar vertebra from each animal was quantified. The primary histomorphometric indices collected were total bone surface, double-labeled surface, interlabel width and eroded surface. From these, the secondary indices were calculated and included percent of double-labeled surface, corrected mineral apposition rate, bone formation rate and percent of eroded surface. The histomorphometric nomenclature conforms with recommendations (Parfitt *et al.* 1987).

Free iron measurement

The iron content in the humeral cortical bone was assayed with EPR spectroscopy (Symons 1978; Kenner *et al.* 2005). Samples were crushed into pieces (< 1 mm) using a mortar and pestle. The granules were defatted with 10 changes of acetone and dried at 60 °C. The samples were then further crushed and sieves used to obtain the 250–600 micrometer fraction. According to a modified protocol (Kenner *et al.* 2005), the free iron EPR measurement, using approximately 100 mg of samples, was made at 24°C with the value for *g*-factor of 2.00541 ± 0.00085 and with the width of 2.5 mT. The signal of free iron was deconvoluted using the Levenberg–Marquardt method (Press *et al.* 1992; Kenner *et al.* 2005). A Bruker 300E spectrometer was used for data collection and instrumental parameters were 25 mW microwave power, 10 mT magnetic field scan width, 0.5 mT magnetic field modulation amplitude, 10^5 receiver gain, 41 ms conversion time, 41 ms time constant, 9.77 GHz microwave frequency and 30 scans.

Chelator synthesis

The synthesis of 1-N-docosyl-triethylenetetraminepentaacetic acid was described previously (Bruenger *et al.* 1992; Miller *et al.* 1993). Briefly, excess triethylenetetramine reacted with 1-docosyl bromide in order to conjugate a single docosyl group to the triethylenetetramine through a primary amino group. Then, exhaustive carboxymethylation of the remaining amino groups was conducted using ethyl bromoacetate with subsequent hydrolysis of the ester. The chelator was characterized and the structure confirmed using ^{1}H- and ^{13}C-NMR and mass spectrometry. The chelator was prepared as HCl salt. All chemicals were purchased from Aldrich and used without further purification.

Statistics

Results were expressed as mean $\pm$ standard error (SE). Data were analyzed using ANOVA followed by a *post hoc* test (Fisher's PLSD) or Student's *t*-test. A 0.1%, 1% or 5% significance level was used and significant differences were considered at $P < 0.05$. The Statview Statistical Package (Abacus Concepts, Inc.) was used for the data analyses.

Results and discussion

We recently reported that the levels of free iron, measured by EPR, that is potentially active for catalyzing free radical formation (Halliwell & Gutteridge 1999) are elevated in osteopenic bones from postmenopausal women and OVX rats (Kenner *et al.* 2005). It is known that excess iron accumulation in individuals with primary or secondary iron-overload disease appears to have a negative impact on skeletal metabolism in these individuals (Brock *et al.* 1994). In other organs such as the heart and brain, there is accumulating evidence for a role of tissue iron in the pathogenesis of atherosclerosis and neurodegenerative diseases, respectively (Rouault 2001; Stadler *et al.* 2004). Furthermore, iron chelation therapies may have some benefit in the treatment of these diseases (Crapper McLachlan *et al.* 1991; Duffy *et al.* 2001). Based on these observations, we hypothesized that the age-associated accumulation of iron in skeletal tissues of postmenopausal

women may have an important role in the pathogenesis of osteoporosis.

To demonstrate our hypothesis, we first confirmed the accumulation of iron in osteopenic bones of OVX rats. The free iron content of cortical bone from OVX rats was determined by the EPR method and found to be significantly greater (22.2%. *t*-test, $P < 0.01$) compared with sham-operated controls. These results suggest an association of increased iron content with the development of osteopenia in this model of estrogen deficiency.

The hypothesis that increased bone iron is associated with the development of osteopenia was further supported by administration of a chelator. The chelator used here (1-N-docosyltriethylenetetraminepentaacetic acid, Figure 1) has a high iron binding affinity and the ability to effectively deplete heavy metals such as plutonium from skeletal and soft tissues in experimental studies (Bruenger *et al*. 1992; Miller *et al*. 1993). Plutonium shares many properties with iron, including coordination chemistry, intracellular pathways and deposition patterns in skeletal tissues (White *et al*. 1988). Following the ovariectomy procedure, the chelator was orally administered. After nine weeks of treatment, the iron content in bones of chelator-treated OVX rats was only 59.8% (*t*-test, $P < 0.01$) of that of the untreated OVX rats, and was 73.0% (*t*-test, $P < 0.01$) of that of the sham control. These results show that chelation therapy can slow or perhaps even reverse the accumulation of iron in bone in both OVX and normally aging rats. Most significantly, however, the reduction of bone iron in the OVX rats by chelation treatment slowed the development of bone loss. This was demonstrated by measuring BMD with pQCT and bone microstructure with Micro-CT.

Because cancellous bone is more susceptible to osteopenia caused by estrogen deficiency, we chose first to measure the BMD in the cancellous bone of the vertebra (Figure 2). The result showed that the

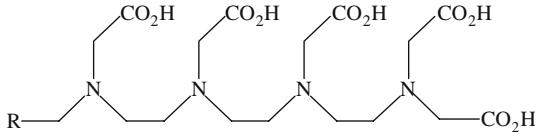

Figure. 1. Chemical structure of 1-N-Docosyltriethylenetetraminepentaacetic acid. It is an amphiphilic and orally active chelator with high iron binding affinity and bone targeting capability ($R = CH_3(CH_2)_{19}CH_2$).

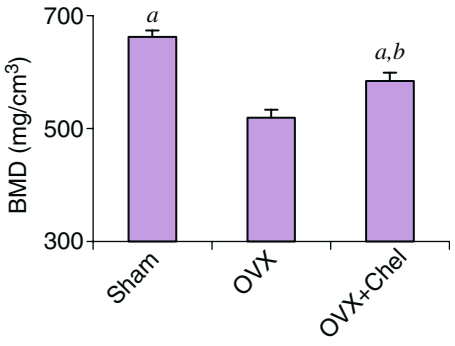

Figure 2. Trabecular BMD measured by pQCT. The trabecular BMD of OVX + Chel and Sham groups were significantly greater than that of OVX group with ANOVA (1% significance level, $^{a}P < 0.002$) and the BMD of Sham group was also significantly greater than that of OVX + Chel group (1% significance level, $^{b}P < 0.004$ by ANOVA). Each group contained six rats. All values were expressed as means ± SE.

average cancellous BMD of chelator-treated OVX rats was significantly greater (12.4%) than that of untreated OVX rats. The average cancellous BMD of untreated OVX rats was 21.6% less than the sham control; while the BMD of the chelator-treated OVX rats was just 11.9% less than that of the sham control. This study suggests that iron chelation treatment slows the loss of cancellous bone mass in estrogen-deficient rats by reducing skeletal iron accumulation.

The structure of the cancellous bone was also examined using the Micro-CT and the derived morphological measurements (Figure 3). The ratio of bone volume to tissue volume (BV/TV) in the chelator-treated OVX rats was significantly higher (9.1%) than that of untreated OVX rats, which indicated more trabecular bone mass in the chelator-treated OVX rats. At the same time, the trabecular separation (Tr. Sp.) was significantly less (10.2%) in the chelator-treated OVX rats compared with the untreated OVX controls. These results show that iron chelation treatment also slows micro-architectural deterioration of cancellous bone following OVX. The increased trabecular bone volume and decreased trabecular separation are evident in the Micro-CT images (Figure 4) of the chelator-treated OVX rats compared with their untreated controls. These results clearly demonstrate a bone preserving action of iron chelation in a model of estrogen deficiency.

In models of iron overload, iron deposits in the bone microenvironment have been associated with impaired bone formation and increased bone

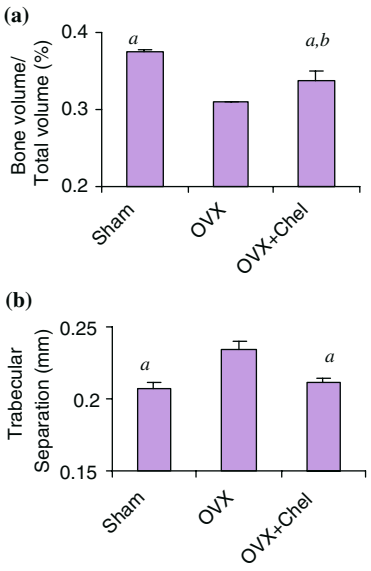

Figure 3. Morphological indices of lumbar vertebral cancellous bone from groups of OVX, OVX + Chel and Sham rats ($n=6$ per group). (a) Trabecular BV/TV measurements of OVX + Chel and Sham groups were significantly greater than that of OVX group with ANOVA (5% significance level, $^{a}P < 0.015$). The BV/TV of Sham group was also significantly greater compared with OVX + Chel group (5% significance level, $^{b}P=0.003$ by ANOVA). (b) Tr. Sp. of OVX + Chel and Sham groups were significantly lower than that of OVX group with ANOVA (0.1% significance level, $^{a}P < 0.0009$). There were no significant differences in Tr. Sp. between OVX + Chel and Sham groups. All values were expressed as means ± SE.

resorption (Isomura *et al*. 2004). The suppression of bone formation with the stimulation of bone resorption would result in the development of osteopenia. Thus, it was hypothesized that iron chelation would reverse some of these putative effects of excess iron on skeletal metabolism. The histomorphometric data showed that the resorption (eroded) surface in the cancellous bone of the chelator-treated OVX rats was about 48% less than that in the untreated OVX rats (Figure 5). There was also a trend ($P > 0.05$ but < 0.1) for a greater cancellous bone formation rate in the chelator-treated animals than in the respective controls. Thus these histomorphometric findings provide a reasonable explanation for the effects of iron reduction on the mitigation of the development of osteopenia in the OVX rat model.

Taken together, the age-associated iron accumulation in bones of OVX rats may play a significant role in the development of bone loss associated with estrogen deficiency. This association is further supported by the observation that by limiting and/or reducing the free iron concentrations in bone by iron chelation, there was a significant retention of bone mass and a slowing of the deterioration of bone structure. The skeletal protection associated with iron reduction by chelation was due to a significant reduction in bone resorption and perhaps a maintenance or even an increase in bone formation after ovariectomy.

Our findings of increased iron with estrogen-deficieny osteopenia and the slowing of the osteopenic changes with iron reduction by chelation, identify a novel therapeutic opportunity to perhaps treat postmenopausal and senile osteoporosis. Due to the side effects associated with traditional hormone replacement therapy, such new therapeutic opportunities may be very important. Moreover, our findings may further help raise awareness about iron nutrition, iron supplements and Western diets that may be associated with excess iron intake and thereby increase the risks of skeletal disease. Whether chelation therapies, as used in this study, would be useful for treatment of diseases that may have an association with iron accumulation appears promising, but clearly requires further studies.

Our findings add further support to the somewhat controversial theory that age-associated iron accumulations in tissues increases the risks of diseases such as atherosclerosis, cancer, diabetes and dementia (Sullivan 1981; Stevens *et al*. 1988; Woo *et al*. 1989; Moirand *et al*. 1997; Rouault 2001). Although there is considerable evidence to support these associations for some diseases, there has been little data presented to suggest a relationship between iron accumulation and skeletal disease, aside from more extreme iron overload situations. The present study supports this general theory by providing evidence for a relationship between iron accumulation and the progression of osteopenia in estrogen-deficiency and aging. Because aging is often accompanied by cancer, atherosclerosis, dementia and osteoporosis, our findings with others suggest that age-associated iron accumulation may, in return, be one of contributing factors for aging. Moreover, our findings may lead to new therapeutic approaches to address a number of aging diseases that are or may be associated with iron accumulation and iron associated oxidative damage.

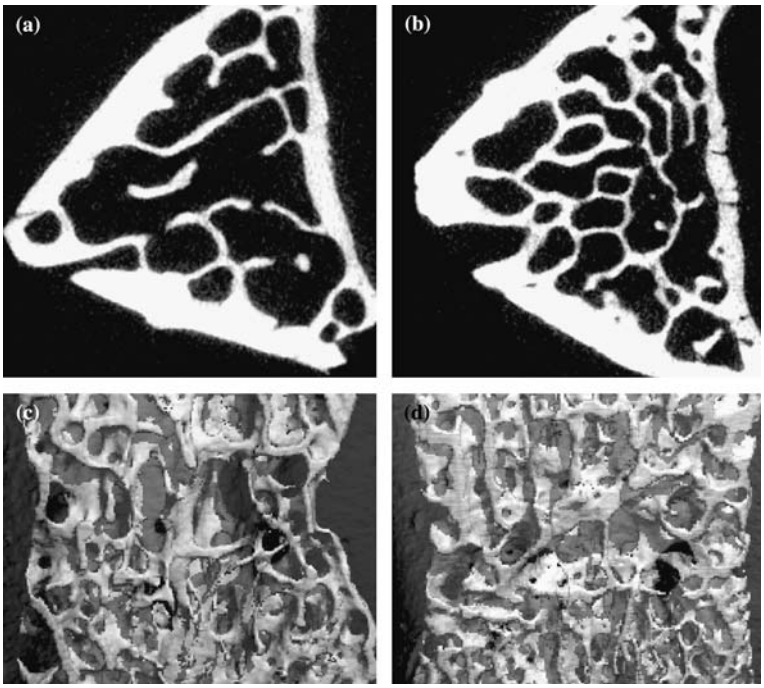

Figure 4. Micro-CT images of the lumbar vertebral body from OVX and OVX + Chel rats. Two-dimensional axial slice (a) OVX and (b) OVX + Chel and three-dimensional reconstruction images (c) OVX and (d) OVX + Chel. The images showed the micro-architectural differences between the groups.

Acknowledgements

We thank B.M. Bowman, J.E. Shea, H. Matsushita and H.Y. Chen for expert assistance, and Scanco for Micro-CT measurement. We also acknowledge Y. Liu for assistance in the preparation of this manuscript. This work was supported by a grant from the NIH (AG021300 awarded to GL).

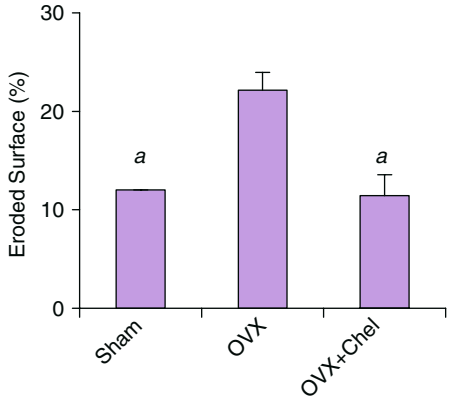

Figure. 5. Dynamic bone histomorphometry. Eroded surfaces (%) of OVX + Chel and Sham groups were significantly lower than that of OVX group with ANOVA (0.1% significance level, $^{a}P < 0.0007$). There were no significant differences in eroded surface between OVX + Chel and Sham groups. Each group contained six animals and all values were expressed as means ± SE.

References

The British Nutrition Foundation 1995. Iron: nutritional and physiological significance: the report of the British Nutrition Foundation's Task Force. First edition, London, New York: Chapman & Hall for the British Nutrition Foundation.

Brock JH, Halliday JW, Pippard MJ and Powell LW (Eds) . 1994 Iron metabolism in health and disease. WB Saunders Co Ltd.;London.

Bruenger FW, Kuswik-Rabiega G, Miller SC. 1992 Decorporation of aged americium deposits by oral administration of lipophilic polyamino carboxylic acids. *J Med Chem* **35**, 112–118.

Crapper McLachlan DR, Dalton AJ, Kruck TP, *et al*. 1991 Intramuscular desferrioxamine in patients with Alzheimer's disease. *Lancet* **337**, 1304–1308.

Cummings SR, Black DM, Rubin SM. 1989 Lifetime risks of hip, Colles', or vertebral fracture and coronary heart disease among white postmenopausal women. *Arch Intern Med* **149**, 2445–2448.

Danesh J, Appleby P. 1999 Coronary heart disease and iron status: meta-analyses of prospective studies. *Circulation* **99**, 852–854.

Department of Health 1998. Nutrition and bone health: with particular reference to calcium and vitamin D. Report of the Subgroup on Bone Health, Working Group on the Nutritional Status of the Population of the Committee on Medical Aspects of Food and Nutrition Policy. London: The Stationery Office. (Report on Health and Social Subjects, No. 49).

Duffy SJ, Biegelsen ES, Holbrook M, *et al*. 2001 Iron chelation improves endothelial function in patients with coronary artery disease. *Circulation* **103**, 2799–2804.

Halliwell B, Gutteridge JM. (1999) Free radicals in Biology and Medicine. Third edition, Oxford University Press.

Howes PS, Zacharski LR, Sullivan J, Chow B. 2000 Role of stored iron in atherosclerosis. *J Vasc Nurs* **18**, 109–114.

Isomura H, Fujie K, Shibata K, *et al*. 2004 Bone metabolism and oxidative stress in postmenopausal rats with iron overload. *Toxicology* **197**, 93–100.

Kato I. Dnistrian AM, Schwartz M, *et al*. 2000 Risk of iron overload among middle-aged women. *Int J Vitam Nutr Res* **70**, 119–125.

Kenner GH, Brik AB, Liu G, *et al*. 2005 Variation of long-lived free radicals responsible for the EPR native signal in bone of aged or diseased human females and ovariectomized adult rats. *Radiat Meas* **39**, 255–262.

Klein RF, Allard J, Avnur Z, *et al*. 2004 Regulation of bone mass in mice by the lipoxygenase gene Alox15. *Science* **303**, 229–232.

Laib A, Kumer JL, Majumdar S, Lane NE. 2001 The temporal changes of trabecular architecture in ovariectomized rats assessed by MicroCT. *Osteoporos Int* **12**, 936–941.

McCance RA, Widdowson EM. 1938 The absorption and excretion of iron following oral and intravenous administration. *J Physiol* **94**, 148–154.

Miller SC, Bruenger FW, Kuswik-Rabiega G, Liu G, Lloyd RD. 1993 Duration and dose-related effects of an orally administered, partially lipophilic polyaminocarboxylic acid on the decorporation of plutonium and americium. *J Pharmacol Exp Ther* **267**, 548–554.

Moirand R, Mortaji AM, Loreal O, Paillard F, Brissot P, Deugnier Y. 1997 A new syndrome of liver iron overload with normal transferrin saturation. *Lancet* **349**, 95–97.

Muhlbauer RC, Li F. 1999 Effect of vegetables on bone metabolism. *Nature* **401**, 343–344.

Parfitt AM, Drezner MK, Glorieux FH, *et al*. 1987 Bone histomorphometry: standardization of nomenclature, symbols, and units. *J Bone Min Res* **2**, 595–610.

Press WH, Teukolsky SA, Vetterling WT, Flannery BP. 1992 Numerical Analysis in C. Cambridge University Press;Cambridge.

Raisz LG, Rodan GA. 2003 Pathogenesis of osteoporosis. *Endocrinol Metab Clin North Am* **32**, 15–24.

Rouault TA. 2001 Iron on the brain. *Nat Genet* **28**, 299–300.

Seidman H, Mushinski MH, Gelb SK, Silverberg E. 1985 Probabilities of eventually developing or dying of cancer–United States, 1985. *CA Cancer J Clin* **35**, 36–56.

Stadler N, Lindner RA, Davies MJ. 2004 Direct detection and quantification of transition metal ions in human atherosclerotic plaques: evidence for the presence of elevated levels of iron and copper. *Arterioscler Thromb Vasc Biol* **24**, 949–954.

Stevens RG, Jones DY, Micozzi MS, Taylor PR. 1988 Body iron stores and the risk of cancer. *N Engl J Med* **319**, 1047–1052.

Sullivan JL. 1981 Iron and the sex difference in heart disease risk. *Lancet* **1**, 1293–1294.

Symons MCR. 1978 Chemical and biochemical aspects of electron spin resonance spectroscopy. Wiley;London.

White DL, Durbin PW, Jeung N, Raymond KN. 1988 Specific sequestering agents for the actinides. 16. Synthesis and initial biological testing of polydentate oxohydroxypyridinecarboxylate ligands. *J Med Chem* **31**, 11–18.

Woo J, Mak YT, Law LK, Swaminathan R. 1989 Plasma ferritin in an elderly population living in the community. *J Med* **20**, 123–134.